Biochemical and Biophysical Research Communications 456 (2015) 926–932

Contents lists available at ScienceDirect

Biochemical and Biophysical Research Communications

journal homepage: www.elsevier.com/locate/ybbrc

Eicosapentaenoic acid (EPA) induced apoptosis in HepG2 cells through ROS–Ca^{2+}–JNK mitochondrial pathways

Yuanyuan Zhang [a], Lirong Han [a], Wentao Qi [b], Dai Cheng [a], Xiaolei Ma [a], Lihua Hou [a], Xiaohong Cao [a,*], Chunling Wang [a,*]

[a] Key Laboratory of Food Nutrition and Safety, Ministry of Education, College of Food Engineering and Biotechnology, Tianjin University of Science and Technology, No. 29, 13th Avenue, Tianjin Economy Technological Development Area, Tianjin 300457, People's Republic of China
[b] Academy of State Administration of Grain, No.11 Baiwanzhuang Avenue, Xicheng District, Beijing, 100037, People's Republic of China

ARTICLE INFO

Article history:
Received 1 December 2014
Available online 18 December 2014

Keywords:
Eicosapentaenoic acid
Apoptosis
ROS
Ca^{2+}
Mitochondrial

ABSTRACT

Eicosapentaenoic acid (EPA), a well-known dietary *n*−3 PUFAS, has been considered to inhibit proliferation of tumor cells. However, the molecular mechanism related to EPA-induced liver cancer cells apoptosis has not been reported. In this study, we investigated the effect of EPA on HepG2 cells proliferation and apoptosis mechanism through mitochondrial pathways. EPA inhibited proliferation of HepG2 cells in a dose-dependent manner and had no significant effect on the cell viability of humor normal liver L-02 cells. It was found that EPA initially evoked ROS formation, leading to $[Ca^{2+}]_c$ accumulation and the mitochondrial permeability transition pore (MPTP) opening; EPA-induced HepG2 cells apoptosis was inhibited by N-acetylcysteine (NAC, an inhibitor of ROS), 1,2-bis (2-aminophenoxy) ethane-N,N,N′,N′-tetraacetic acid (BAPTA-AM, a chelator of calcium) and CsA (inhibitor of MPTP). The relationship between ROS production, the increase of cytoplasmic Ca and MPTP opening was detected. It seems that ROS may act as an upstream regulator of EPA-induced $[Ca^{2+}]_c$ generation, moreover, generation of ROS, overload of mitochondrial $[Ca^{2+}]_c$, and JNK activated cause the opening of MPTP. Western blotting results showed that EPA elevated the phosphorylation status of JNK, processes associated with the ROS generation. Simultaneously, the apoptosis induced by EPA was related to release of cytochrome C from mitochondria to cytoplasm through the MPTP and activation of caspase-9 and caspase-3. These results suggest that EPA induces apoptosis through ROS–Ca^{2+}–JNK mitochondrial pathways.

1. Introduction

Hepatocellular carcinoma (HCC) is the third most common cause of death from cancer [1,2]; surgery is the treatment of choice for only the small fraction of patients. In such a high death rate and low cure rate, it is very imperative to find effective agents for treatment of cancer.

Polyunsaturated fatty acids (PUFAs) are considered as important bioactive sources; they have been suggested as natural products that may play significant roles in modulating cancer development [3].

Eicosapentaenoic acid (EPA) is a typical dietary *n*−3 PUFAs, a group of fatty acids characterized by a double bond that sits three carbons down from the n terminal of the molecule [4–6]; it retards the growth and development of breast, colon, and liver cancer and leukemia in vitro and in vivo [7]. EPA could inhibit the MCF-7 cell growth by 30% [8]; Chiu et al. identified that reduction of bcl-2 expression may be an important step during the EPA-induced only in HL-60 but not K-562 cells apoptosis. However, the mechanisms related to HepG2 cells apoptosis induced by EPA have not been elucidated.

Induction of apoptosis and inhibition of cell proliferation are recognized as a valuable tool for preventing and treating cancers [9]. Mitochondria undergo an initial priming phase associated with hyperpolarisation which leads to an effector phase during apoptosis; meanwhile, mitochondria swell and release cytochrome C. The mitochondrial pathway of apoptosis is associated with the generation of reactive oxygen species, the release of cytochrome C, cytoplasmic calcium concentration and the opening of the permeability transition (PT) pore. However, few studies have focused on the relationship between the generation of reactive oxygen species, cytoplasmic calcium concentration and the opening of the permeability transition (PT) pore. Bcl-2 exerts effects on the mitochondria and can promote the release of cytochrome C into the cytosol from the mitochondria [10,11]. Activation of downstream caspase-3 is regulated by cytochrome C and caspase-9.

* Corresponding authors. Fax: +86 022 60601428.
E-mail addresses: caoxh@tust.edu.cn (X. Cao), wangchunling@tust.edu.cn (C. Wang).

http://dx.doi.org/10.1016/j.bbrc.2014.12.036
0006-291X/

In this paper, in order to investigate the influence of EPA induced apoptosis in HepG2 cells. The apoptosis mechanism was investigated. The cytoplasmic calcium concentration, the reactive oxygen species in mitochondria, release of cytochrome C, and increases in activation of cleaved caspase-9 and caspase-3 proteins induced by EPA were also tested. The expressions of phospho-JNK after EPA treatment were measured. Furthermore, bcl-2 in the process of apoptosis was also tested. Our results showed that EPA induced mitochondrial-dependent apoptosis referred to cytoplasmic calcium concentration, the reactive oxygen species and phospho-JNK MAPK pathway. EPA induced the increase expression of caspase-3 protein that mediated apoptosis.

2. Materials and methods

2.1. Materials

Eicosapentaenoic acid (EPA) and 3-(4, 5-dimethylthiazol-2-yl)-2, 5-diphenyl tetrazolium bromide (MTT) were purchased from Sigma (St. Louis, MO, USA). Penicillin- streptomycin solution, trypsin, phosphate buffered saline (PBS) and dimethyl sulfoside side (DMSO) were purchased by Thermo (Beijing, China). NAC (inhibitor of ROS), BAPTA-AM (1, 2-bis (2-aminophenoxy) ethane-N,N,N′,N′-tetraacetic acid, the intracellular Ca^{2+} chelator), CsA (inhibitor of MPTP) and the molecular probe of DCFH-DA, Flou-3/AM and calcein-AM were also purchased from Sigma (St. Louis, MO, USA). The phospho-JNK, JNK, bcl-2, cytochrome C, caspase-3, caspase-9, β-actin and horseradish peroxidase-conjugated secondary antibodies were purchased from Santa Cruz Biotechnology (Santa Cruz, CA, USA). JNK inhibitor (SP200125) was obtained from Cal Biochem (San Diego, CA, USA). All other chemicals were of the highest commercial grade available.

2.2. Cell culture

Human hepatoma (HepG2) cell lines were obtained from the Institute of Biochemistry and cell Biology (Shanghai, China). The cells were maintained in Minimum Essential Medium Alpha Medium (DMEM, high glucose) (Solarbio, Beijing, China) supplemented with 10% fetal bovine serum (Gibco BRL, Grand Island, NY, USA), 100 units/ml penicillin and 0.1 mg/ml streptomycin at 37 °C in a humidified chamber of 95% air and 5% CO_2 atmosphere.

2.3. MTT assay for cell viability

Before harvesting, the cells were incubated with 20 μl 3-(4, 5-dimethylthiazol-2-yl)-2, 5-diphenyl tetrazolium bromide (MTT) in medium for 4 h at 37 °C. The viable cells convert the MTT to formazan, which generates a blue-purple color after dissolving in 150 μl dimethyl sulphoxide (DMSO). The absorbance at 570 nm was the measured with a microplate reader (Model 680, Bio-Rad, Hercules, CA, USA). All experiments were carried out in triplicate. Cell viability (%) = [(absorbance of cells treated with EPA)/absorbance of control cells] × 100%.

2.4. Fluorescent staining of HepG2 cell nuclei (AO/EB)

Acridine orange and ethidium bromide (AO/EB) staining (Solarbio, Beijing, China) was carried out as previously described [12]. Briefly, HepG2 cells in the exponential growth phase were seeded in 24-well culture plates at a final concentration of 1×10^5 cells/well. Cells were treated with 75 μM EPA for various times and then stained with the staining solution containing 100 μg/ml acridine orange and 100 μg/ml ethidium bromide for 20 min at room temperature in the dark. Cells were observed under an inverted fluorescence microscope (AMG, USA) after the staining.

2.5. Measurement of ROS production

The intracellular ROS generation was measured as previously described [12]. HepG2 cells were incubated with 75 μM EPA and treated with 10 μM DCFH-DA for 30 min at 37 °C in the dark. Then the cells were washed three times with PBS (pH 7.2). The fluorescence intensity was measured by laser scanning confocal microscope (LSCM) (Nikon, D-Eclipse C1, Tokyo, Japan) using an excitation of 488 nm and an emission of 525 nm (at a detection spectrum of 488 nm).

2.6. Measurement of cytoplasmic calcium concentration ($[Ca^{2+}]_c$)

With Fluo-3 acetoxymethyl ester (Fluo-3/AM) as a fluorescent Ca^{2+} indicator, cytoplasmic $[Ca^{2+}]_c$ change was measured by LSCM according to a previously described method [13]. HepG2 cells were treated with 75 μM EPA, and then incubated with Fluo-3/AM for 1 h at 37 °C in the dark, washed with PBS (pH 7.2) thrice. The change of fluorescence intensity was measured by LSCM using an excitation of 488 nm and an emission of 525 nm.

2.7. Measurement of mitochondrial permeability transition pore (MPTP) activity

Considering the positive correlation between the EPA applied and the ROS generation, Ca^{2+} accumulation, MPTP opening, the activity of MPTP was mediated in succession. In brief, cells were cultured and treated with 75 μM EPA for various times, then incubated with calcein-AM and $CoCl_2$ for 1 h at 37 °C in the dark. Cells were washed with PBS (pH 7.2) twice and the fluorescence was measured with excitation at 488 nm and emission at 525 nm.

2.8. Western blot analysis

To investigate the potential apoptotic induction mechanism, the expression of characteristic apoptosis protein was measured by Western blot. The protocol was described previously [14] and probed with the primary antibodies (Santa Cruz, CA, USA). The membranes were washed extensively and incubated with the appropriate secondary antibodies conjugated to horseradish peroxidase (Amersham Pharmacia Biotech). The immunoreactive bands were detected with a DAB kit (Zhong-shan Goldenbridge, Beijing, China). Densitometry of the western blot bands was scanned (Chemidoc, Bio-Rad, Hercules, CA, USA). Each test was performed in triplicate experiments [14].

2.9. Statistical analysis

The data are presented as the means ± S.E., and each experiment was repeated at least three times. Statistical analysis was performed using the SPSS software (version 18.0) to determine the significant differences. All values were analysed by one-way analysis of variance (ANOVA) followed by a post hoc Tukey's test for multiple comparisons. Values of $P < 0.05$ were considered statistically significant.

3. Result

3.1. EPA-induced cell viability and morphological changes of HepG2 cells

As shown in Fig. 1A, EPA had an outstanding suppression HepG2 cells proliferation in a does-dependent and time-dependent

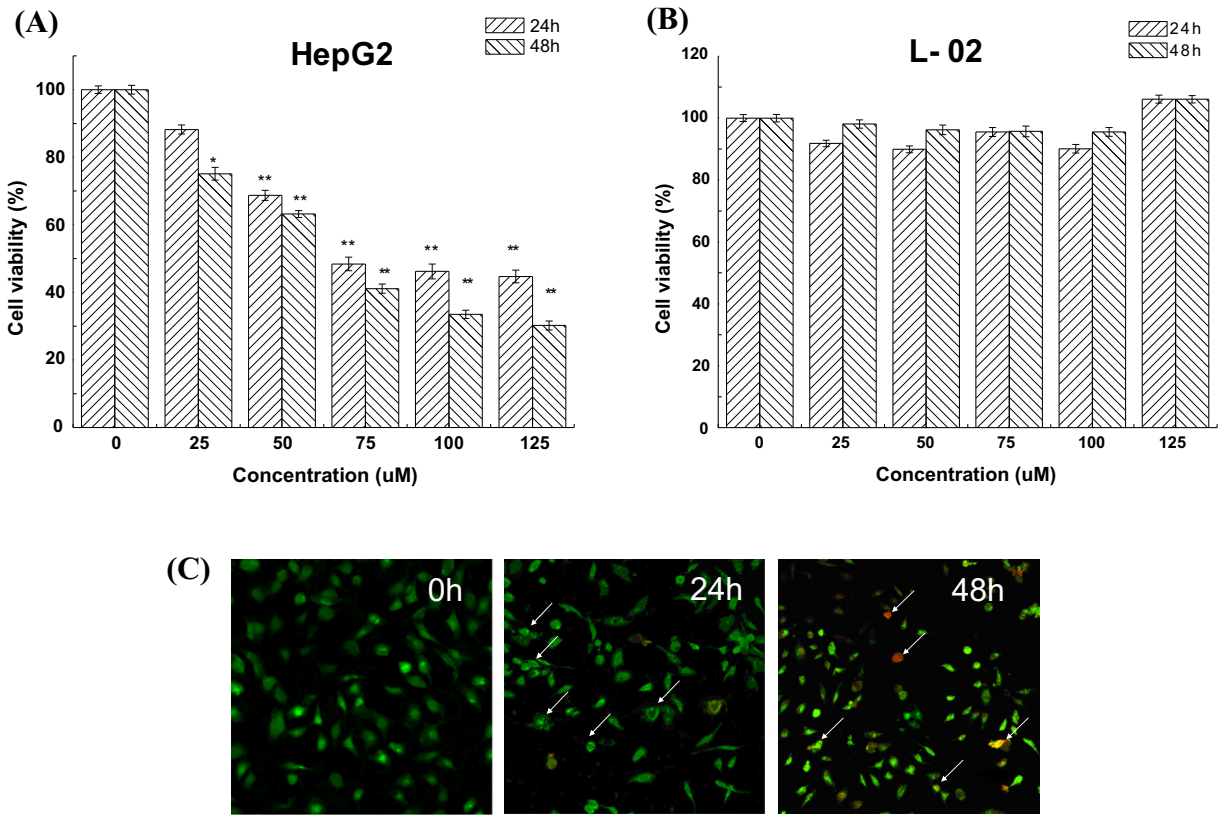

Fig. 1. EPA-induced cell viability and morphological changes of HepG2 cells. The viability of cells was determined by MTT assay. Morphological changes in HepG2 cells were measured by AO/EB staining. Effect of various concentrations of EPA (0, 25, 50, 75, 100 and 125 μM) on cell viability in HepG2 cells (A) or L-02 cells (B) for 24 h and 48 h ($^{*}P < 0.05$, $^{**}P < 0.01$ vs. the control group). The control group was the untreated cells which were incubated with 0 μM EPA. Each bar is representative of three independent experiments, and data were analysed by ANOVA and Duncan's multiple range tests. (C) Cell morphology change was recorded by a fluorescence microscope (400×).

manner. At the concentration of 75 μM, the inhibition rate at 24 h was about 51.6%; at the concentration of 100 μM, the inhibition rate at 48 h reached about 70%. In contrast (Fig. 1B), EPA had no obvious effect on L-02 cells from 24 h to 48 h after treatment. These results indicated that EPA specially inhibited the HepG2 cells proliferation, whereas it had no significant effect on the somatic cells, such as L-02 cells.

In the absence of EPA, HepG2 cells were normal in size and structure and the staining pattern of cells was uniformly green in both nuclei and plasma (Fig. 1C). By contrast, cells treated with EPA for 24 h revealed marked nuclear condensation, and nuclear shrinkage, all of which were characteristics of programmed cell death (as arrow illustrated). Meanwhile, at the longer time 48 h, cells revealed obviously apoptosis shape and necrosis was also observed (red). These results indicated that EPA can induce apoptosis in HepG2 cells.

3.2. Measurement of intracellular ROS production, cytoplasmic calcium concentration ($[Ca^{2+}]_c$) and MPTP activation

To determine whether EPA has an effect on the intracellular ROS generation, HepG2 cells were treated with 75 μM EPA for 0 h, 12 h, 24 h and 48 h, respectively. As shown in Fig. 2A and B, the DCFH-DA fluorescence gradually increased in a time-dependent manner. The change of fluorescence increased significantly at 24 h, and reached the peak value at 48 h. In addition, the apoptotic rate was measured by FCM as shown in Fig. 2C. NAC (an inhibitor of ROS pretreatment could reverse EPA-induced apoptosis from 17.21% to 8.29%, and it confirmed that ROS indeed was involved in EPA induced apoptosis.

The measurement of $[Ca^{2+}]_c$ of the cells was determined by LSCM with fluorescent probe Fluo-3/AM. As shown in Fig. 2D and E, HepG2 cells revealed significant strong $[Ca^{2+}]_c$ fluorescence intensity at 12 h, and reached the peak value at 48 h, simultaneously, these increases of $[Ca^{2+}]_c$ were in a time- dependent manner. After that, 20 μM BAPTA-AM (the chelator of calcium) was used to incubated cells prior to adding EPA; it could significantly inhibit the EPA-induced apoptosis, and the apoptosis rate decreased from 17.21% to 7.31% (Fig. 2F). The above results support our hypothesis that EPA treatment leads to an increase in Ca^{2+} production, which may represent a critical step in EPA-induced apoptosis in HepG2 cells.

The prior results indicated that EPA could induce cell apoptosis in HepG2 cells. We hypothesized that EPA-induced apoptosis of HepG2 cells through a mitochondrial-dependent pathway. As shown in Supplementary Fig. 1A, the fluorescence of calcein-AM in cytoplasm was gradually decline in a time-dependent manner. The change of fluorescence decreased significantly at 24 h, and reached the peak value at 48 h (Supplementary Fig. 1B). The effect of CsA (MPTP inhibitor) on cell apoptosis was tested. HepG2 cells were treated with 75 μM EPA for 24 h in the presence and absence of CsA (50 μM). As shown in Supplementary Fig. 1C, CsA could inhibit the cell apoptosis which induced by EPA.

3.3. Measurement of MAPKs

ROS may lead to the activation of MAPKs [15,16]. To determine whether MAPK are involved in EPA-induced apoptosis, the expression of the phosphorylated forms of JNK was analyzed by Western blot analysis. HepG2 cells were pretreated with 2 mM NAC and

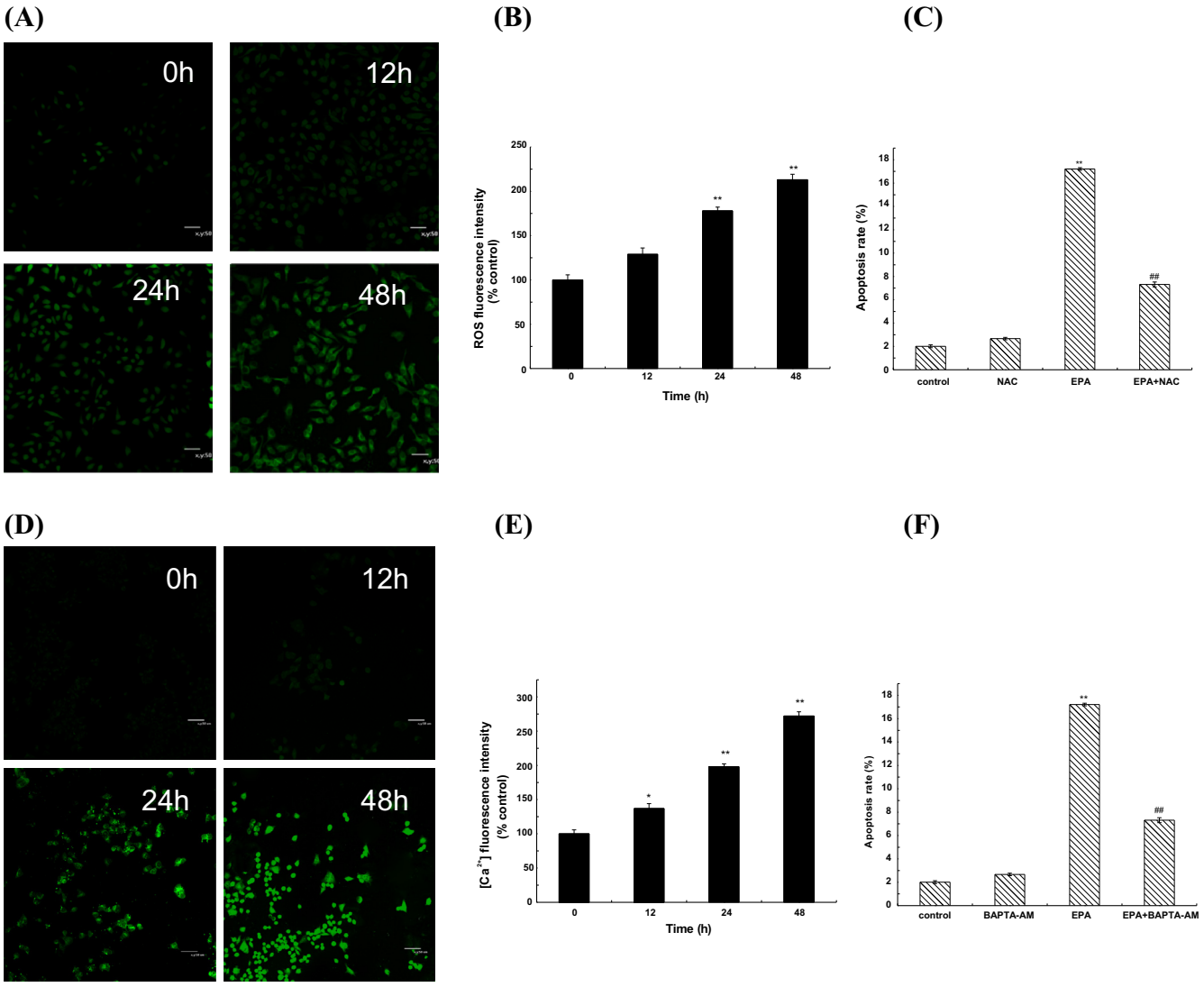

Fig. 2. Intracellular ROS production, cytoplasmic calcium concentration ($[Ca^{2+}]_c$) and the activity of MPTP in EPA (75 μM) treatment HepG2 cells. Visualization of the DCFH-DA (A) and $[Ca^{2+}]_c$ (D) fluorescence in EPA treatment HepG2 cells was recorded by using a LSCM, bar = 50 μm (200×). Changes of the DCFH-DA (B) and $[Ca^{2+}]_c$ (E) fluorescence intensity in HepG2 cells ($^{**}P < 0.01$ vs. the control group). Effect of the NAC (C) and BAPTA-AM (F) on EPA-induced cell apoptosis. The apoptotic rate of cells was measured by FCM in the presence or absence of 2 μM NAC and 20 μM BAPTA-AM. ($^{**}P < 0.01$ compared with the control group; $^{\#\#}P < 0.01$ compared with EPA alone.) Each bar is representative of three independent experiments, and data were analysed by ANOVA and Duncan's multiple range tests.

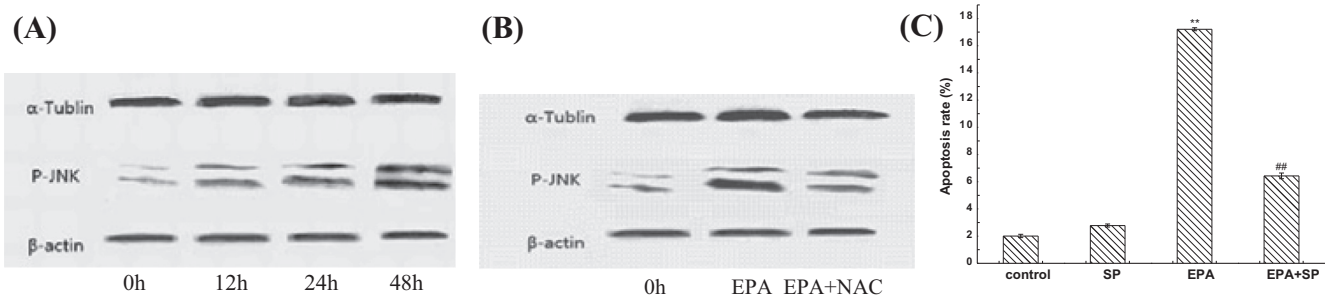

Fig. 3. Measurement of MAPK subfamily in EPA (75 μM) treatment HepG2 cells. (A) Effect of EPA on phosphorylation of JNK in HepG2 cells. (B) Effect of EPA and the antioxidant NAC on activation of MAPK subfamily proteins JNK in HepG2 cells. Cells were treated with 75 μM EPA for 0 h and 24 h in the presence or absence of 2 mM NAC. The expression of protein was analyzed by western bolt. β-Actin was used as an equal loading control. (C) Effect of JNK inhibitor SP600125 on EPA-induced cell apoptosis. Cells were treated with 75 μM EPA for 24 h in the presence or absence of 5 μM SP600125. The apoptotic rate of cells was estimated by FCM. ($^{**}P < 0.01$ compared with the control group; $^{\#\#}P < 0.01$ compared with EPA alone.) Each bar is representative of three independent experiments, and data were analysed by ANOVA and Duncan's multiple range tests.

then incubated with 75 μM EPA for 24 h. As shown in Fig. 3(A) and (B), the levels of phosphorylated JNK increased in a time-dependent manner, and NAC pretreatment could block EPA-induced phosphorylated JNK. These result showed that JNK may be targets of ROS and the ROS–JNK pathway is involved in EPA-induced apoptosis. To further explore the functional involvement of JNK activation in EPA-induced apoptosis, the JNK inhibitor SP600125 (SP) was used for treating HepG2 cells with EPA. The result suggested that SP600125 (SP) reversed the cytotoxic effect of EPA (Fig. 3(C)). Overall, the results indicated that the activation of JNK was associated with EPA-induced apoptosis in HepG2 cells.

3.4. Relationship between $[Ca^{2+}]_c$, ROS and MPTP

Above results indicated that cytoplasmic calcium concentration ($[Ca^{2+}]_c$) increase, ROS generation, MPTP opening and activation of JNK were involved in EPA-induced apoptosis. In order to further investigate the relationship between them, cells were respectively preincubated with NAC (2 mM), BAPTA-AM (20 μM) and SP600125 (5 μM) prior to adding EPA (75 μM), and then measured the fluorescent intensity of Fluo-3/AM, DCFH-DA and calcein-AM. The increase of $[Ca^{2+}]_c$ was effectively blocked by NAC (Fig. 4A). However, BAPTA-AM had no obvious effect on ROS increase (Fig. 4B). These results seems that $[Ca^{2+}]_c$ generation was dependent on the ROS increase, and it also could lead us to hypothesize that ROS may act as an upstream regulator of EPA-induced $[Ca^{2+}]_c$ generation. In addition, the fluorescence intensity of calcein in HepG2 cells which were pretreated with these inhibitors was respectively increased (Fig. 4C). It indicated that these inhibitors could inhibit MPTP open position and reverse apoptosis rate in HepG2 cells that incubated with 75 μM EPA.

3.5. Effect of EPA on cytochrome C and caspases

It was well known that bcl-2 is an inhibiting apoptosis gene; the release of cytochrome C from the intermembrane spaces of the mitochondria into the cytosol is very vital to the cell apoptosis via a mitochondrial-dependent pathway [17,18]. The expression of Bcl-2 was decreased in a time-dependent manner; cytochrome C expression decreased in mitochondria and simultaneously accumulated in the cytoplasm in a time-dependent manner (Supplementary Fig. 2A). The changes of the cytochrome C proteins were prevented by CsA (Supplementary Fig. 2B). Above results indicated that the opening of MPTP was induced by EPA, then cytochrome C releasing from mitochondria to cytoplasm is a time-dependent manner.

The caspase-cascade was initiated by activated upstream caspase, eventually led to cell apoptosis[19,20]. As shown in Supplementary Fig. 2C, the expression levels of pro-caspase-9 and pro-caspase-3 were all decreased in a time-dependent manner, indicating that EPA induced the degradation of the pro-caspase-9 and pro-caspase-3 in HepG2 cell.

4. Discussion

Polyunsaturated fatty acids (PUFAs) have been suggested due to their modulatory activities on cancer cell growth [21,22]. PUFAs, particularly those found in fish oils, have been found to inhibit

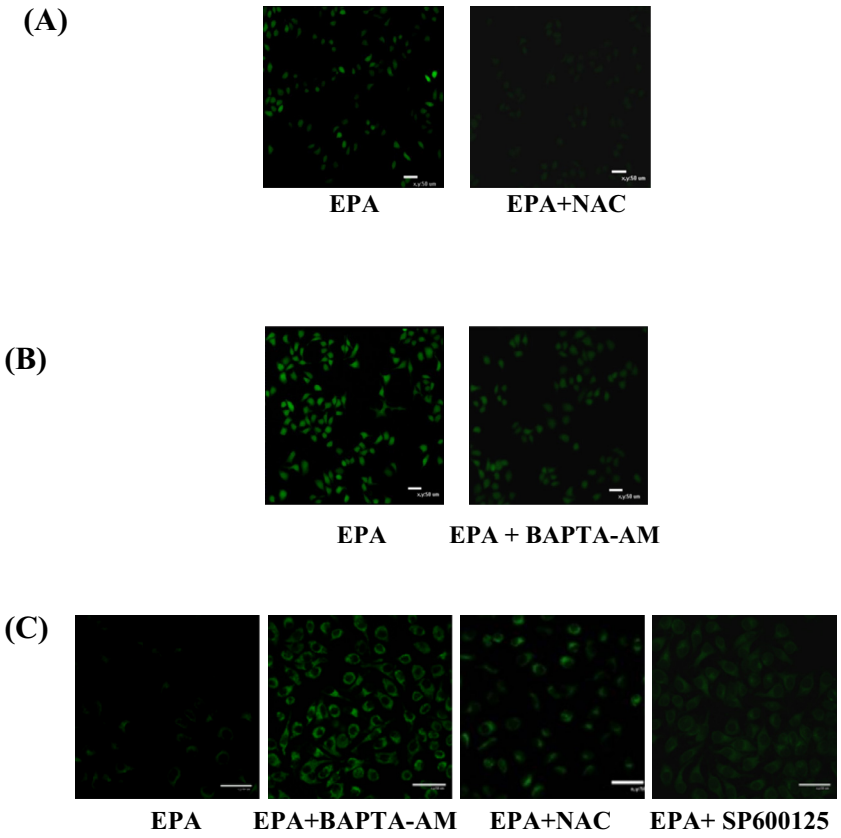

Fig. 4. The relationship between intracellular cytoplasmic calcium concentration ($[Ca^{2+}]_c$) increase, ROS production and MPTP opening. HepG2 cells were treated with 75 μM EPA in the presence and absence of 2 mM NAC, 20 μM DAPTA-AM and 5 μM SP600125. Visualization of the DCFH-DA (A), Fluo-3/AM (B) calcein-AM (C) fluorescence was recorded by using a LSCM, bar = 50 μm (200×).

proliferation in vitro. EPA was selected as a representative $n-3$ PUFAs from fish oil; it has been shown previously as effective anti-cancer PUFAs [23,24]. As the mechanisms of PUFAs inhibiting tumor cells were different and the inhibitory mechanisms were very complex, the present study determines to investigate the underlying anti-tumor activities and mechanisms of EPA in HepG2 cells. Our results indicated that cell viability had a dose dependent relationship with EPA concentration respectively. EPA could inhibit cell growth and induce apoptosis in HepG2 cells. But the mechanisms responsible for apoptosis induced by EPA appear to be not investigated.

It is known that cell apoptosis leads to characteristic changes in cell morphology, including cell shrinkage, chromatin condensation and nuclear fragmentation [25]. Most of the studies declared that cell apoptotic was related to the production of reactive oxygen species which was generated in mitochondrial respiratory chain. The intracellular free Ca^{2+} seems to be essentially involved in the mechanism of apoptosis [26–28]. In the present study, both the $[Ca^{2+}]_c$ and the ROS production in HepG2 cells induced by EPA increased gradually in a time dependent manner. Moreover, the results indicated that $[Ca^{2+}]_c$ elevation was depended on the ROS generation.

Furthermore, prolonged MPTP opening due to mitochondrial Ca^{2+} overload can result in apoptosis [29]. It could lead to mitochondria depolarization and oxidative phosphorylation uncoupling [30]. Our data show that MPTP opening was induced by EPA, which associated with increasing of $[Ca^{2+}]_c$, ROS generation and activation of JNK, finally leading to apoptosis in HepG2 cells.

Activated MAPK can transmit extracellular signals to regulate cell growth, proliferation, differentiation, migration, apoptosis and so on [31]. The mitogen activated protein kinase (MAPK) signaling plays a key role in the outcome and the sensitivity to anti-cancer therapies. To further elucidate the molecular events associated with EPA induced apoptotic signals, we examined the proteins relevant to apoptosis. It showed that EPA-induced the phosphorylation of JNK in HepG2 cells, whereas pretreatment with NAC clearly antagonized this effect.

Bcl-2, which acts as a typical inhibiting apoptosis gene, has been shown to govern mitochondrial apoptosis pathway by preventing the efflux of cytochrome C and other pro-apoptotic factors [32]. Cytochrome C releasing from mitochondrial into cytoplasm dues to the MPTP opening and the disruption of mitochondrial while apoptotic process executed by intrinsic pathway. There are some characteristic proteins involves in these two apoptosis pathways: the intrinsic pathway activates caspase-9, the extrinsic pathway activates caspase-8 [33]. Furthermore, active caspase-9 triggers a caspase cascade, such as caspase-3, to induce cell apoptosis [34]. In our present study, the mechanism of intrinsic pathway was mainly concerned. The results showed that EPA- induced ROS causes apoptosis in HepG2 cells through ROS and JNK activation regulated mitochondrial-dysfunction triggered cytochrome C and caspase-9, caspase-3 activation.

In summary, these results above showed that EPA could directly induce cell apoptosis, which was mediated by ROS production, $[Ca^{2+}]_c$ increase, activation of JNK and MPTP opening regulated cytochrome C release from mitochondria, caspase-9 and caspase-3 in HepG2 cell. Overload of mitochondrial $[Ca^{2+}]_c$, generation of ROS and JNK activated caused the opening of MPTP, cytochrome C and Ca^{2+} efflux to cytoplasm, eventually lead to apoptosis. Taken together, our data suggest that accumulation of ROS induced by EPA evokes cytoplasmic $[Ca^{2+}]_c$ and the MPTP opening. A speculated schematic diagram of EPA-induced cell apoptosis is depicted in Supplementary Fig. 3. There is important new insights into the possible molecular mechanisms of EPA, in addition to its potential value as a novel candidate as an anti-tumor agent. However, these results are not sufficient to characterize the essential behavior of EPA. Further studies could focus on the novel pathway of cell apoptosis.

Acknowledgment

This work was supported by these projects in China (2012BAD33B04, 13JCZDJC29800, 31000768, 2012AA022108, 2012GB2A100016, 2013AA102106, 10ZCZDSY07000, 31171731 and IRT1166).

Appendix A. Supplementary data

Supplementary data associated with this article can be found, in the online version, at http://dx.doi.org/10.1016/j.bbrc.2014.12.036.

References

[1] B.E.S. Hashem, K.L. Rudolph, Hepatocellular carcinoma: epidemiology and molecular carcinogenesis, J. Gastroenterol. 132 (2007) 2557–2576.
[2] J. Whang Peng, A.L. Cheng, C. Hsu, C.M. Chen, Clinical development and future direction for the treatment of hepatocellular carcinoma, J. Exp. Clin. Med. 2 (2010) 93–103.
[3] C. Galli, R. Butrum, Dietary omega 3 fatty acids and cancer: an overview, World Rev. Nutr. Diet 66 (1991) 446–461.
[4] Hajime Ishii, Yasuo Horie, Shigetoshi Ohshima, et al., Eicosapentaenoic acid ameliorates steatohepatitis and hepatocellular carcinoma in hepatocyte-specific Pten-deficient mice, J. Hepatol. 50 (2009) 562–571.
[5] Y.A. Carpentier, L. Portois, W.J. Malaisse, N-3 fatty acids and the metabolic syndrome, Am. J. Clin. Nutr. 83 (2006) 1499S–1504S.
[6] G. Schmitz, J. Ecker, The opposing effects of n-3 and n-6 fatty acids, Prog. Lipid Res. 47 (2008) 147–155.
[7] H. Chamras, A. Ardashian, D. Heber, J.A. Glaspy, Fatty acid modulation of MCF-7 human breast cancer cell proliferation, apoptosis and differentiation, J. Nutr. Biochem. 13 (2002) 711–717.
[8] M. Murata, H. Kaji, K. Iida, Y. Okumura, K. Chihara, Dual action of eicosapentaenoic acid in hepatoma cells, J. Biol. Chem. 33 (2001) 31422–31430.
[9] S.M. Kornblau, The role of apoptosis in the pathogenesis, prognosis, and therapy of hematologic malignancies, Leukemia 12 (1998) S41–S46.
[10] F. Radogna, S. Cristofanon, L. Paternoster, M. D'Alessio, M.D. Nicola, C. Cerella, et al., Melatonin antagonizes the intrinsic pathway of apoptosis via mitochondrial targeting of Bcl-2, Pineal Res. 44 (2008) 316–325.
[11] S. Cory, D.C. Huang, J.M. Adams, The Bcl-2 family: roles in cell survival and oncogenesis, Oncogene 22 (2003) 8590–8607.
[12] X.H. Cao, A.H. Wang, C.L. Wang, et al., Surfactin induces apoptosis in human breast cancer MCF-7 cells through a ROS/JNK-mediated mitochondrial/caspase pathway, Chem. Biol. Interact. 183 (2010) 357–362.
[13] C.L. Wang, T.B. Ng, X.H. Cao, Y. Jiang, Z.K. Liu, T.Y. Wen, F. Liu, CLP induces apoptosis in human leukemia K562 cells through Ca^{2+} regulating extracellular-related protein kinase ERK activation, Cancer Lett. 2 (2009) 221–227.
[14] X. Cao, A.H. Wang, R.Z. Jiao, C.L. Wang, D.Z. Mao, L. Yan, et al., Surfactin induces apoptosis and G2/M arrest in human breast cancer MCF-7 cells through cell cycle factor regulation, Cell Biochem. Biophys. 55 (2009) 163–171.
[15] C. Vasutakarn, Y. Sanvarinda, C. Sukumal, Reactive oxygen species production and MAPK activation are implicated in tetrahydrobiopterin-induced SH-SY5Y cell death, Neurosci. Lett. 3 (2009) 178–182.
[16] A.k. Hirakawa, N.S. Takeyama, T.S. Nakatani, T. Tanaka, Mitochondrial permeability transition and cytochrome release in ischemia–reperfusion injury of the rat liver, J. Surg. Res. 2 (2003) 240–247.
[17] C. Lee, D.W. Park, J. Lee, T.I. Lee, Y.J. Kim, Y.S. Lee, et al., Secretory phospholipase A2 induces apoptosis through TNF-a and cytochrome c-mediated caspase cascade in murine macrophage RAW 264.7 cells, Eur. J. Pharmacol. 536 (2006) 47–53.
[18] V. Senthil, S. Ramadevi, V. Venkatakrishnan, et al., Withanolide induces apoptosis in HL-60 leukemia cells via mitochondria mediated cytochrome c release and caspase activation, Chem. Biol. Interact. 1 (2007) 19–30.
[19] P.H. Andrew, What is the mitochondrial permeability transition pore?, J Mol. Cell. Cardiol. 6 (2009) 821–831.
[20] M. José, H. Garcí a, D.M. Irene, et al., Nitration of tyrosine 74 prevents human cytochrome c to play a key role in apoptosis signaling by blocking caspase-9 activation, BBA-Bioenerg. 1797 (2010) 981–993.
[21] R.A. Karmali, L. Adams, J.R. Trout, Plant and marine n-3 fatty acids inhibit experimental metastasis of rat mammary adenocarcinoma cells, Prostaglandins Leukot. Essent. Fatty Acids 48 (1993) 309–314.
[22] M. Noguchi, M. Minami, R. Yagasaki, et al., Chemoprevention of DMBA-induced mammary carcinogenesis in rats by low-dose EPA and DHA, Br. J. Cancer 75 (1997) 348–353.
[23] P.B.S. Lai, J.A. Ross, K.C.H. Fearon, J.D. Anderson, D.C. Carter, Cell cycle arrest and induction of apoptosis in pancreatic cancer cells exposed to eicosapentaenoic acid in vitro, Br. J. Cancer 74 (1996) 1375–1383.

[24] X.H. Liu, D.P. Rose, Suppression of type IV collagenase in MDA-MB-435 human breast cancer cells by eicosapentaenoic acid in vitro and in vivo, Cancer Lett. 92 (1995) 21–26.
[25] S.H. Kaufmann, M.O. Hengartner, Programmed cell death: alive and well in the new millennium, Trends Cell Biol. 11 (2001) 526–534.
[26] H.U. Simon, A.H. Yehia, F.L. Schaffer, Role of reactive oxygen species (ROS) in apoptosis induction, Apoptosis 5 (2000) 415–418.
[27] D.J. McConkey, S. Orrenius, The role of calcium in the regulation of apoptosis, J. Leukoc. Biol. 59 (1996) 775–783.
[28] K.R. Martin, J.C. Barrett, Reactive oxygen species as double-edged swords in cellular processes: low-dose cell signaling versus high-dose toxicity, Hum. Exp. Toxicol. 21 (2002) 71–75.
[29] J. Yang, X. Liu, K. Bhalla, et al., Prevention of apoptosis by Bcl-2: release of cytochrome c from mitochondria blocked, Science 275 (1997) 1129–1132.
[30] A.P. Halestrap, S.J. Clarke, S.A. Javadov, Mitochondrial permeability transition pore opening during myocardial reperfusion – a target for cardioprotection, Cardiovasc. Res. 61 (2004) 372–385.
[31] T.A. Khavari, J. Rinn, Ras/Erk MAPK signaling in epidermal homeostasis and neoplasia, Cell Cycle 6 (2007) 2928–2931.
[32] R.M. Kluck, E. Bossy-Wetzel, D.R. Green, D.D. Newmeyer, The release of cytochrome c from mitochondria: a primary site for Bcl-2 regulation of apoptosis, Science 275 (1997) 1132–1136.
[33] Seongho Ryu, Shih-chieh Lin, Nadia Ugel, Marco Antoniotti, Bud Mishra, Mathematical modeling of the formation of apoptosome in intrinsic pathway of apoptosis, Syst. Synth. Biol. 2 (2008) 49–66.
[34] H.E. Kim, F. Du, M. Fang, X. Wang, Formation of apoptosome is initiated by cytochrome c-induced dATP hydrolysis and subsequent nucleotide exchange on Apaf-1, Proc. Natl. Acad. Sci. 102 (2005) 17545–17550.